

# Three-dimensional free vibration analysis of thick laminated circular plates

Sumit Khare<sup>1\*</sup>, N. D. Mittal<sup>2</sup>

<sup>1,2</sup>Department of Mechanical Engineering, Maulana Azad National Institute of Technology, Bhopal-462003, INDIA  
<sup>\*</sup>Corresponding Author: e-mail: sumitkhare8686@gmail.com, Tel +91-8109152818

---

## Abstract

In this communication, a numerical analysis regarding free vibration of thick laminated circular plates, having free, clamped as well as simply-supported boundary conditions at outer edges of plates is presented. The employment of finite element is made in this communication. The finite element methodology operates on the basis of three-dimensional theory of elasticity and was employed to assess the natural frequencies for laminated circular plates of various thickness-to-outer radius ratios. The first five natural modes of flexural vibrations for different boundary conditions are presented in pictorial forms. Verification of the accuracy of the results was made using the necessary convergence analysis and checked using literature results.

*Keywords:* Laminated Composite Circular Plate; Natural Frequency; Mode Shape; Finite Element Method.

DOI: <http://dx.doi.org/10.4314/ijest.v8i2.2>

---

## 1. Introduction

Laminated circular plates are commonly used structural component having a broad application in aerospace, civil, mechanical, nuclear, electronic as well as marine engineering. An essential prerequisite in designing and performance assessment of mechanical systems is understanding the free vibration behavior of different plate components. The dynamic response of complex engineering systems is intimately linked with plate response frequencies as well as vibration mode shapes. A thorough analysis of free vibration data is often useful in arriving at the resonant behavior and fatigue stress estimation at vulnerable machine locations.

A comprehensive survey of early investigation on free vibration studies of circular plates carried out by Leissa (1969) as well as Liew et al. (1995) noted that classical thin plate theory (CTPT) and Mindlin plate theory were majorly applied by investigators. It is understood that CTPT, which ignores the influences of transverse shear deformation as well as normal strain, overestimate the vibration frequencies and error increases with plate thickness. However, various shear deformation as well as higher-order theories which include the shear deformation and normal strain, have been proposed in the computations concerning thick plates during the past few decades. Rao and Prasad (1975) analysed the natural vibrations of annular plates considering the influences of shear deformation as well as rotatory inertia. Irie et al. (1982) presented the vibration characteristics of Mindlin annular plates in nine groupings of free, simply supported and clamp boundary condition of inner and outer edge conditions using Bessel function.

Also, Liew et al.(2000),Wu et al.(2002) , Han and Liew (1999) and Wang (2004) discussed the free vibration of circular, annular and sector plates employing differential quadrature method based on the classical thin plate theory or Mindlin plate theory. Lin and Tseng (1998) studied the free vibration characteristics of polar orthotropic laminated circular and annular plates by using a finite element method having first order shear deformation theory. Hosseini-Hashemi et al. (2010) provided an precise closed-form frequency equation for thick circular plates using a third-order shear deformation theory. Hosseini-Hashemi et al. (2012) presented an precise closed-form solution for free flexural vibration of thick laminated circular plates with an attached rigid core using the first-order shear deformation theory. Senjanovic (2014) utilised the modified Mindlin theory to examine the free vibration of thick circular plates. Sharma (2014) investigated the free vibration problem involving averagely thick antisymmetric laminated annular sector plates having edge-supports that are elastic established on first order shear deformation theory using the differential quadrature method. Powmya and Narasimhan (2015) studied the free vibration behavior of polar orthotropic circular as well as annular plates by Chebyshev collocation technique based on first order shear deformation theory.

The analysis of relatively thick plates is a challenging task. Most two – dimensional theories, if applied for the analysis of such thick plates, result in significant errors due to their inherent limitations. Such theories are almost always based on some simplifying assumptions and consequently offer a great deal of convenience in analysis. The expressions, thus obtained are simple in nature and easy to work with but are likely to be error prone in some cases. A three dimensional analysis, though more complicated, succeeds in getting rid of these errors to a considerable extent and goes far beyond a typical two – dimensional analysis in terms of utility, accuracy and extractable information. The three – dimensional research endeavors listed in literature are relatively few and the reasons are pretty understandable.

So and Leissa (1998), Zhou et al. (2003), Kang and Liessa (1998), Liew and Yang (1999,2000) and Kang (2003) presented the three-dimensional method of analysis for free vibration of circular as well as annular plates employing Ritz method. Liu and Lee (2000) employed the finite element method to investigate three-dimensional vibrations of thick circular and annular plates. Malekzadeh (2010) analysed the three-dimensional free vibration analysis of thick functionally graded annular plates influenced by the thermal environment. The three-dimensional analyses of circular and annular plates resting on Pasternak elastic foundation and Winkler foundation studied by Liew et al.(1996), Zhou et al. (2006), Hashemi et al. (2008). Houmat (2004) investigated the free vibration of annular sector plates employing finite element scheme. Komur et.al (2010) has conducted a buckling analysis for laminated composite plates having an elliptical/circular hole centered in the plate using finite element method (FEM) using ANSYS finite element software. Chen and Ren (1998) studied the transverse vibration of thin circular and annular plates with variable thickness using finite element method. Liang et al. (2007) used three-node annular finite elements to compute the natural frequencies of circular annular plates of polar orthotropy and non-uniform thickness. Ranjan and Ghosh (2009) studied the free and forced Transverse vibration behavior of a thin spinning disk having distributed patch attached to it as well as discrete point masses at the periphery of plate using finite element analysis. Malekzadeh (2010) analysed a three-dimensional elasticity solution system, which addressed the free vibration analysis of thick-laminated circular and annular plates, which rested on two-parameter elastic foundation. In this paper the effects of different fiber orientation angle, thickness to radii ratio, with free, clamped and simply-supported boundary conditions of plates on the free vibration responses are discussed in detail using finite element scheme, with roots in three-dimensional theory of elasticity. Verification of accuracy as well as the numerical reliability was made using standard convergence principles while the study was compared with those existing in literature.

**2. The basic formulations**

Consider a thick, laminated annular plate having inner radius  $R_1$ , outer radius  $R_2$ , total thickness  $h$  and fiber orientation angle  $\beta$ . An orthogonal cylindrical coordinates  $(r, \theta, z)$  are used as depicted in Figure 1, where  $u, v$  and  $w$  denotes the displacement of any point of the plate in the  $r, \theta$  and  $z$  direction, respectively.

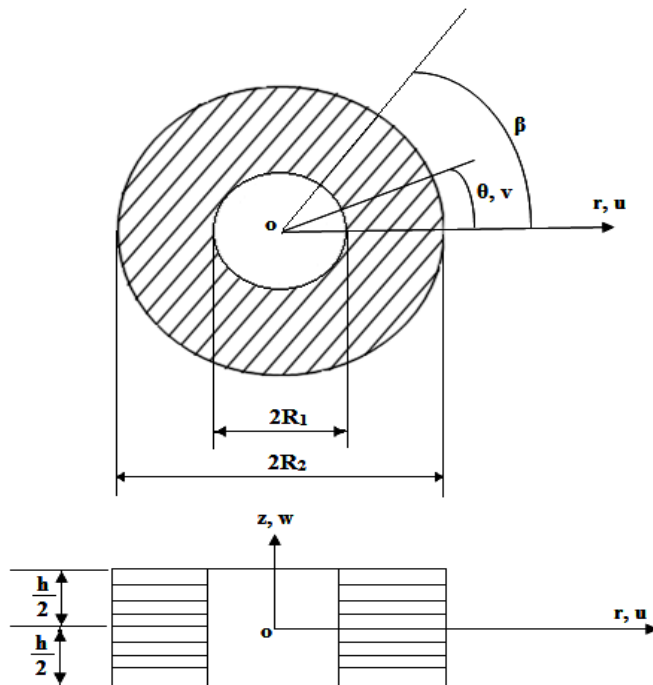


**Figure 1** Geometry and coordinate system of the annular plate

The displacement field that satisfy the three-dimensional elasticity equation of motion of circular plates, designated by  $u$ ,  $v$ , and  $w$  are assumed as

$$\begin{aligned}
 u &= U(r, z, t) \cos n\theta \\
 v &= V(r, z, t) \sin n\theta \\
 w &= W(r, z, t) \cos n\theta,
 \end{aligned}
 \tag{1}$$

where  $n$  and  $t$  represent the wave numbers (circumferential) as well as time, respectively. The displacements are afterwards used in the strain-displacement associations while the strains are consequently stated with respect to displacements. The stress-strain expressions sequentially direct to stresses that are as well stated with respect to displacements (Liu and Lee , 2000).

The constitutive relations representing that of arbitrary lamina for annular plate may be stated as,

$$\begin{Bmatrix} \sigma_z \\ \sigma_\theta \\ \sigma_r \\ \tau_{r\theta} \\ \tau_{rz} \\ \tau_{\theta z} \end{Bmatrix} = \begin{bmatrix} C_{11} & C_{12} & C_{13} & 0 & 0 & C_{16} \\ C_{12} & C_{22} & C_{23} & 0 & 0 & C_{26} \\ C_{13} & C_{23} & C_{33} & 0 & 0 & C_{36} \\ 0 & 0 & 0 & C_{44} & C_{45} & 0 \\ 0 & 0 & 0 & C_{45} & C_{55} & 0 \\ C_{16} & C_{26} & C_{36} & 0 & 0 & C_{66} \end{bmatrix} \begin{Bmatrix} \epsilon_z \\ \epsilon_\theta \\ \epsilon_r \\ \epsilon_{r\theta} \\ \epsilon_{rz} \\ \epsilon_{\theta z} \end{Bmatrix},
 \tag{2}$$

where  $[C]$  is the material stiffness matrix (Malekzadeh , 2010).

The Hamilton's principle is required for the modeling of vibrating plates using finite element (Liu and Lee, 2000):

$$0 = \int_0^t \int_{vol} \left[ (\sigma_r \delta \epsilon_r + \sigma_z \delta \epsilon_z + \sigma_\theta \delta \epsilon_{r\theta} + \tau_{z\theta} \delta \epsilon_{z\theta} + \tau_{r\theta} \delta \epsilon_{r\theta} + \tau_{rz} \delta \epsilon_{rz}) - (\dot{u} \delta \dot{u} + \dot{v} \delta \dot{v} + \dot{w} \delta \dot{w}) \right] dv dt,
 \tag{3}$$

here,  $\dot{u}$ ,  $\dot{v}$  as well as  $\dot{w}$  represent velocity constituents along the three co-ordinates. Following the substitution of stresses as well as strains obtained through strain-displacement as well as stress-strain associations into above stated expression, we conclude with a variational kind in which the only main variables are the three displacements. The universal procedure of the finite element scheme then follows. If a single finite element becomes utilized in the integration, the element equation may be obtained as

$$[m] \{\dot{U}\} + [k] \{U\} = 0$$

here,  $\{U\}^T = [U_1, U_2, \dots, U_m, V_1, V_2, \dots, V_m, W_1, W_2, \dots, W_m]$ ,  $m$  refers to number of nodes in an element,  $[m]$  and  $[k]$  are the element mass and stiffness matrices.

The universal expression of motion may be obtained through the assembly of all the element expressions:

$$[M] \{\ddot{X}\} + [K] \{X\} = 0$$

which corresponds to an eigenvalue equation of the following form:

$$[K] \{x\} = \lambda [M] \{x\} = 0$$

The eigenvalue  $\lambda$  represents the square of vibration frequency  $\omega$  and eigenvector  $\{x\}$  denotes the corresponding mode shape.

3. Material and methods

A finite element analysis was made for obtaining the first five natural frequencies using three-dimensional ‘SOLID185’ of ANSYS. In addition, SOLID185 Structural Solid is appropriate for modeling common 3-D solid structures. As demonstrated in figure 2, the element contains eight nodes with three degrees of freedom at each node: translations in the nodal x, y, and z directions. (ANSYS Inc., 2009). The Block-Lanczos algorithm is utilised in free vibration analysis of thick laminated circular plates (Figure 3).

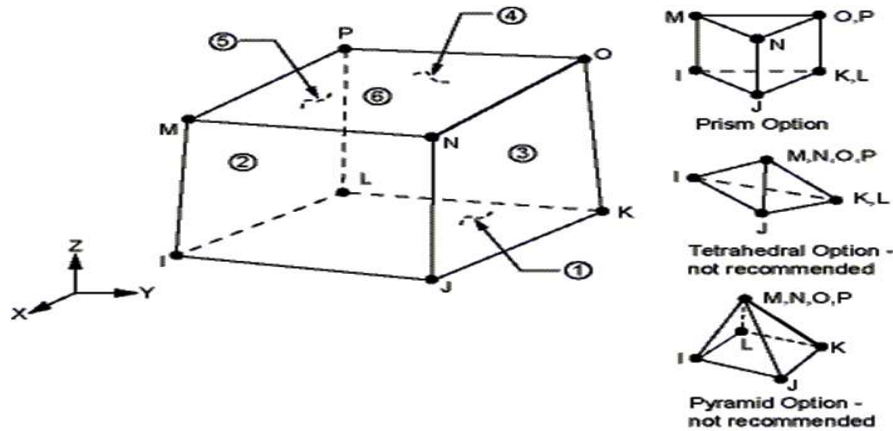


Figure 2 Eight noded SOLID185 element

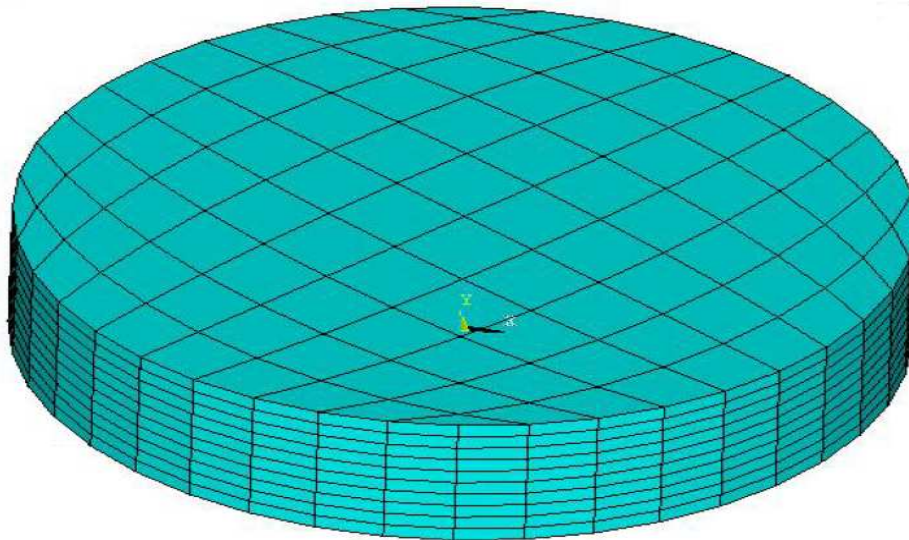


Figure 3 Finite element model of a thick laminated circular plate

Mechanical properties of glass/epoxy laminated plates are listed in Table 1.

Table 1. Mechanical properties of the glass/epoxy laminated plates (Reddy, 2004)

$E_1$ (GPa)	$E_2$ (GPa)	$G_{12}$ (GPa)	$G_{13}$ (GPa)	$G_{23}$ (GPa)	$\nu$
53.781	17.927	8.9635	8.9635	4.4475	0.25

**4. Results and Discussion**

The current investigation was primarily validated via performing convergence study of non-dimensional frequency parameter  $\Omega$  defined by  $\Omega = \omega R_2^2 \sqrt{\rho h / D}$ , where  $D = Eh^3 / 12(1 - \nu^2)$ , of isotropic circular plates ( $\nu = 1/3$ ) with respect to number of elemental divisions (N) as well as through matching up of current results with literature reported cases. The number in parenthesis (n, s) indicates the number of nodal diameters n, in the  $s^{th}$  mode of vibration. The rate of convergence of the first five frequency parameters for isotropic circular plates with clamped, simply supported and free boundary conditions are presented in Table 2-4, for thickness-radius ratios varying from 0.1 to 0.5 in step of 0.1. It can be seen from that N=15, is sufficient to obtain satisfactory convergence for first five frequency parameters.

**Table 2.** Convergence behavior of the first five frequency parameter  $\Omega = \omega R_2^2 \sqrt{\rho h / D}$  for isotropic circular plate with clamped boundary condition

N	Mode number (n, s)				
	1(0,0)	2(1,0)	3(2,0)	4(0,1)	5(3,0)
<b>(a) <math>h/R_2=0.1</math></b>					
7	10.4283	21.7720	35.5635	42.1115	51.8218
9	10.4826	21.7897	35.6348	43.0988	51.6304
11	10.2066	21.0863	34.0250	40.1456	48.7675
13	10.0848	20.6712	33.2306	38.4154	47.5493
15	10.0424	20.5753	33.0433	37.9726	47.3433
17	10.0253	20.4796	33.0105	37.7931	47.2276
<b>(b) <math>h/R_2=0.2</math></b>					
7	9.8278	18.8888	29.1105	33.6838	40.2617
9	9.6245	18.8009	29.0413	34.0394	40.0299
11	9.4536	18.4006	28.2071	32.4892	38.6473
13	9.3676	18.1593	27.7543	31.5463	37.9937
15	9.3421	18.1025	27.652	31.2997	37.8875
17	9.3275	18.0371	27.6322	31.1883	37.8137
<b>(c) <math>h/R_2=0.3</math></b>					
7	8.6985	16.0522	23.7183	27.0007	31.8281
9	8.6739	15.9754	23.6418	27.1761	31.6365
11	8.5511	15.7110	23.1393	26.2463	30.8234
13	8.4871	15.5522	22.8576	25.6635	30.4271
15	8.4673	15.5135	22.7934	25.5069	30.36
17	8.4557	15.4683	22.7798	25.4341	30.3115
<b>(d) <math>h/R_2=0.4</math></b>					
7	7.7703	13.6761	19.6995	22.1995	26.0189
9	7.7439	13.6095	19.6308	22.3029	25.8622
11	7.6528	13.4285	19.2916	21.6759	25.0356
13	7.6040	13.3172	19.0994	21.2753	25.0356
15	7.5883	13.2889	19.0545	21.1650	24.9871
17	7.5791	13.2566	19.0442	21.1132	24.9517
<b>(e) <math>h/R_2=0.5</math></b>					
7	6.9352	11.7888	16.7370	18.7443	21.9125
9	6.9094	11.7318	16.6768	18.3830	21.7812
11	6.8397	11.5998	16.4258	18.3494	21.3643
13	6.8016	11.5169	16.2832	18.0496	21.1580
15	6.7887	11.4950	16.2492	17.9655	21.1196
17	6.7812	11.4705	16.2406	17.9372	21.0914

**Table 3.** Convergence behavior of the first five frequency parameter  $\Omega = \omega R_2^2 \sqrt{\rho h / D}$  for isotropic circular plate with simply supported boundary condition.

N	Mode number (n, s)				
	1(0,0)	2(1,0)	3(2,0)	4(0,1)	5(3,0)
<b>(a) h/R<sub>2</sub>=0.1</b>					
7	4.9780	14.0886	25.9652	31.1872	40.6181
9	5.0141	14.1190	26.0418	31.8331	40.3566
11	4.9346	13.8138	25.1410	30.0928	38.6387
13	4.8952	13.6254	24.7280	29.1561	37.9233
15	4.8794	13.5871	24.6232	28.9016	37.7744
17	4.8758	13.5502	24.6017	28.8128	37.6903
<b>(b) h/R<sub>2</sub>=0.2</b>					
7	4.8456	13.1048	23.0095	27.1966	34.2712
9	4.8419	13.0538	22.9288	27.4563	33.9390
11	4.7968	12.8488	22.3488	26.3701	32.8608
13	4.7730	12.7277	22.0613	25.7400	32.3697
15	4.7642	12.6999	21.9910	25.5725	32.2699
17	4.7606	12.6699	21.9742	25.5015	32.2031
<b>(c) h/R<sub>2</sub>=0.3</b>					
7	4.6730	11.9584	20.0081	23.3332	28.6238
9	4.6618	11.8998	19.9151	23.4829	28.3460
11	4.6257	11.7400	19.4929	22.7166	27.5939
13	4.6061	11.6458	19.2783	22.2578	27.2437
15	4.5991	11.6232	19.2259	22.1347	27.1717
17	4.5957	11.5982	19.2128	22.0797	27.1217
<b>(d) h/R<sub>2</sub>=0.4</b>					
7	4.4682	10.8215	17.3870	20.0849	24.1838
9	4.4550	10.7668	17.3148	20.1833	23.9580
11	4.4240	10.6387	16.9951	19.6131	23.4031
13	4.4068	10.5626	16.8302	19.2643	23.1421
15	4.4006	10.5449	16.7894	19.1691	23.0873
17	4.3975	10.5229	16.7787	19.1259	23.0485
<b>(e) h/R<sub>2</sub>=0.5</b>					
7	4.2481	9.7844	15.2516	17.4708	20.7694
9	4.2346	9.7356	15.1757	17.54	20.5818
11	4.2072	9.6308	14.9252	17.0965	20.1516
13	4.1918	9.5681	14.7947	16.8207	19.9484
15	4.1863	9.5345	14.7619	16.744	19.9047
17	4.1834	9.5345	14.7528	16.709	19.8732

**Table 4.** Convergence behavior of the first five frequency parameter  $\Omega = \omega R_2^2 \sqrt{\rho h / D}$  for isotropic circular plate with free boundary condition

N	Mode number (n, s)				
	1(2,0)	2(0,0)	3(3,0)	4(1,0)	5(4,0)
<b>(a) h/R<sub>2</sub>=0.1</b>					
7	5.3340	8.9708	12.3127	20.2938	21.6057
9	5.3287	8.9616	12.2800	20.2753	21.4854
11	5.3043	8.9216	12.1943	20.0464	21.2480
13	5.2816	8.8750	12.1476	19.9561	21.1588
15	5.2808	8.8593	12.1191	19.8716	21.0441
17	5.2505	8.8220	12.0455	19.7307	20.8762

**Table 4 (cont'd).** Convergence behavior of the first five frequency parameter  $\Omega = \omega R_2^2 \sqrt{\rho h / D}$  for isotropic circular plate with free boundary condition

N	Mode number (n, s)				
	1(2,0)	2(0,0)	3(3,0)	4(1,0)	5(4,0)
<b>(b) <math>h/R_2=0.2</math></b>					
7	5.1450	8.5817	11.5491	18.5019	19.5704
9	5.1406	8.5756	11.5380	18.5006	19.4733
11	5.1221	8.5363	11.4515	18.3073	19.2975
13	5.1128	8.5183	11.4210	18.2823	19.2284
15	5.0995	8.4908	11.3541	18.1420	19.0353
17	5.0851	8.4683	11.3080	18.0471	18.9218
<b>(c) <math>h/R_2=0.3</math></b>					
7	4.9285	8.1022	10.6575	16.5271	17.3937
9	4.9250	8.0972	10.6293	16.5270	17.3172
11	4.8947	8.0380	10.5143	16.2691	17.0355
13	4.8888	8.0262	10.4915	16.2565	16.9841
15	4.8773	8.0030	10.4411	16.1549	16.8300
17	4.8641	7.9802	10.3929	16.0595	16.7340
<b>(d) <math>h/R_2=0.4</math></b>					
7	4.6658	7.5353	9.6766	14.5250	15.2375
9	4.6623	7.5404	9.5458	14.5258	15.1787
11	4.6402	7.4959	9.5760	14.3488	14.9984
13	4.6357	7.4866	9.5581	14.3406	14.9597
15	4.6261	7.4679	9.5210	14.2675	14.8657
17	4.6156	7.4490	9.4833	14.1950	14.7787
<b>(e) <math>h/R_2=0.5</math></b>					
7	4.4078	7.0170	8.8254	12.8306	13.5307
9	4.3946	6.9974	8.7678	12.7707	13.4038
11	4.3823	6.9698	8.7312	12.6750	13.3186
13	4.3736	6.9542	8.6976	12.6378	13.2480
15	4.3657	6.9389	8.6696	12.5840	13.1788
17	4.3560	6.9213	8.6351	12.5214	13.1018

**Table 5.** Comparison of the first five frequency parameter  $\Omega = \omega R_2^2 \sqrt{\rho h / D}$  for isotropic circular plate with different boundary condition

h/R <sub>2</sub>	Mode number (n, s)				
	1 (0,0)	2 (1,0)	3 (2,0)	4 (0,1)	5 (3,0)
<b>(a) Clamped circular plates</b>					
0.1	10.0424	20.5753	33.0433	37.9726	47.3433
[Mindlin <sup>a</sup> ]	9.94	20.23	32.41	36.48	-
[3-D Ritz <sup>b</sup> ]	9.9909	20.297	32.43	36.744	46.14
[Reddy's TPT <sup>c</sup> ]	9.94614	20.1993	32.2634	36.5489	45.8905
0.2	9.3421	18.1025	27.652	31.2997	37.8875
[Mindlin <sup>a</sup> ]	9.24	17.83	27.21	30.21	-
[3-D Ritz <sup>b</sup> ]	9.3225	17.963	27.366	30.649	37.338
[Reddy's TPT <sup>c</sup> ]	9.26503	17.855	27.2148	30.4749	37.1513
0.3	8.4673	15.5135	22.7934	25.5069	30.3600
[Mindlin <sup>a</sup> ]	8.36	15.26	22.38	24.64	-
[3-D Ritz <sup>b</sup> ]	8.4676	15.453	22.667	25.15	30.093
[Reddy's TPT <sup>c</sup> ]	8.4113	15.385		25.1011	30.0729

<sup>a</sup> Irie et al. (1982)

<sup>b</sup> Liew and Yang (1999)

<sup>c</sup> Hosseini-Hashemi et al. (2010)

**Table 5 (cont'd).** Comparison of the first five frequency parameter  $\Omega = \omega R_2^2 \sqrt{\rho h / D}$  for isotropic circular plate with different boundary condition

h/R <sub>2</sub>	Mode number (n, s)				
	1 (0,0)	2 (1,0)	3 (2,0)	4 (0,1)	5 (3,0)
0.4	7.5883	13.2889	19.0545	21.1650	24.9871
[Mindlin <sup>a</sup> ]	7.47	13.04	18.64	20.42	-
[3-D Ritz <sup>b</sup> ]	7.6002	13.27	19.001	20.951	24.84
0.5	6.7887	11.4950	16.2492	17.9655	21.1196
[3-D Ritz <sup>b</sup> ]	6.8068	11.497	16.229	17.825	21.029
(b) Simply supported circular plates					
0.1	4.8794	13.5871	24.6232	28.9016	37.7744
[Mindlin <sup>a</sup> ]	4.89	13.52	24.41	28.24	-
[3-D Ritz <sup>b</sup> ]	4.8975	13.58	24.555	28.31	37.472
[Reddy's TPT <sup>c</sup> ]	4.89421	13.5142	24.3263	28.2547	36.9926
0.2	4.7642	12.6999	21.9910	25.5725	32.2699
[Mindlin <sup>a</sup> ]	4.78	12.67	21.92	24.99	-
[3-D Ritz <sup>b</sup> ]	4.7876	12.764	22.13	25.188	32.389
[Reddy's TPT <sup>c</sup> ]	4.77871	12.6324	21.7279	25.0414	31.6336
0.3	4.5991	11.6232	19.2259	22.1347	27.1717
[Mindlin <sup>a</sup> ]	4.6	11.6	19.18	21.59	-
[3-D Ritz <sup>b</sup> ]	4.6234	11.723	19.453	21.879	-
[Reddy's TPT <sup>c</sup> ]	4.60704	11.6491	18.2838	21.6757	27.1569
0.4	4.60704	10.5449	16.7894	19.1691	23.0873
[Mindlin <sup>a</sup> ]	4.4006	10.5449	16.7894	19.1691	23.0873
[3-D Ritz <sup>b</sup> ]	4.40	10.51	16.74	18.66	-
0.5	4.6253	10.6620	17.0450	18.9940	-
[3-D Ritz <sup>b</sup> ]	4.1863	9.5345	14.7619	16.744	19.9047
(c) Free circular plates					
0.1	5.2808	8.8593	12.1191	19.8716	21.0441
[Mindlin <sup>a</sup> ]	5.28	8.87	-	19.71	-
[3-D Ritz <sup>b</sup> ]	5.2795	8.872	12.074	19.738	20.831
[Reddy's TPT <sup>c</sup> ]	5.27842	8.8688	12.0675	19.7172	-
0.2	5.0995	8.4908	11.3541	18.1420	19.0353
[Mindlin <sup>a</sup> ]	5.11	8.51	-	17.98	-
[3-D Ritz <sup>b</sup> ]	5.1185	8.5194	11.337	18.056	18.882
[Reddy's TPT <sup>c</sup> ]	5.11607	8.50842	11.3233	17.9983	-
0.3	4.8773	8.0030	10.4411	16.1549	16.8300
[Mindlin <sup>a</sup> ]	4.89	8.01	-	15.98	-
[3-D Ritz <sup>b</sup> ]	4.9005	8.0344	10.439	16.102	16.75
[Reddy's TPT <sup>c</sup> ]	4.89609	8.01507	10.4176	16.0153	-
0.4	4.6261	7.4679	9.5210	14.2675	14.8657
[Mindlin <sup>a</sup> ]	4.64	7.46	-	14.09	-
[3-D Ritz <sup>b</sup> ]	4.651	7.5008	9.5294	14.241	14.806
0.5	4.3657	6.9389	8.6696	12.5840	13.1788
[3-D Ritz <sup>b</sup> ]	4.3913	6.9727	8.6854	12.578	13.145

<sup>a</sup> Irie et al. (1982)

<sup>b</sup> Liew and Yang (1999)

<sup>c</sup> Hosseini-Hashemi et al. (2010)

The comparison studies are also carried out here in Table 5, for circular plate with different boundary conditions, in order to examine the discrepancies between the present finite element solution and Mindlin plate solution (Irie et al., 1982), 3-D Ritz



solution (Liew and Yang, 1999) and Reddy’s third-order plate theory solution (Hosseini-Hashemi et al., 2010). The comparisons show good agreement with most of differences being less than 2%.

On the basis of above verification of the current approach, results of convergence behavior of the first five frequency parameters  $\Omega = \omega R_2^2 \sqrt{\rho h / D_o}$  where  $D_o = E_1 h^3 / 12 (1 - \nu_{12} \nu_{21})$ , for glass/epoxy laminated circular plates with thickness-radius ratios varying from 0.1 to 0.5 in step of 0.5 under different boundary condition are presented in Table 6-8. It can be seen that N=15, is sufficient to obtain satisfactory convergence for first five frequency parameters of glass/epoxy laminated circular plates. It is seen that the first axisymmetric flexural mode (0, 0), is found to be lowest fundamental mode except when the boundaries of the circular plates are free, for which it is found corresponding to mode type (2, 0).

**Table 6.** Convergence of the first five frequency parameters  $\Omega = \omega R_2^2 \sqrt{\rho h / D_o}$  for glass/epoxy laminated circular plate with clamped boundary condition ( $\theta=30^\circ$ )

N	Mode number (n, s)				
	1(0,0)	2(1,0)	3(2,0)	4(0,1)	5(3,0)
(a) $h/R_2=0.1$					
7	8.3874	16.3859	26.0089	31.6059	37.0811
9	8.2632	16.0596	25.5660	31.6003	36.3772
11	8.1931	15.8208	25.1543	30.3425	34.9085
13	8.2300	15.7119	24.5106	29.1863	34.0940
15	8.1020	15.9851	24.2491	28.3471	33.9547
17	8.0980	15.7762	24.2969	28.1901	33.9401
(b) $h/R_2=0.2$					
7	7.4086	13.4218	19.9487	23.3156	26.3882
9	7.2497	13.0520	19.5856	23.3176	25.7000
11	7.2543	13.0372	19.3658	22.6315	25.4753
13	7.3078	13.03199	19.1947	22.2186	25.1737
15	7.1669	13.1066	18.9193	21.6903	25.2061
17	7.1586	13.0356	18.9016	21.5810	25.0928
(c) $h/R_2=0.3$					
7	6.3889	10.9119	15.5775	17.808	19.8686
9	6.2320	10.5662	15.3035	17.8741	19.7728
11	6.2713	10.6475	15.1564	17.3843	19.3774
13	6.3247	10.6737	15.1200	17.2210	19.2303
15	6.1890	10.6305	14.9014	16.8999	19.3194
17	6.1706	10.6149	14.8636	16.7987	19.1709
(d) $h/R_2=0.4$					
7	5.4987	9.0334	12.604	14.2456	15.793
9	5.3552	8.7255	12.3986	14.3448	15.7495
11	5.4074	8.8372	12.2893	13.946	15.4773
13	5.4564	8.8717	12.2812	13.8732	15.3801
15	5.3342	8.7836	12.1203	13.6708	15.4904
17	5.3084	8.7838	12.0818	13.5726	15.3416
(e) $h/R_2=0.5$					
7	4.7716	7.6485	10.5269	11.8264	13.0627
9	4.6436	7.3764	10.3698	11.9373	13.0384
11	4.6981	7.4922	10.2816	11.5932	12.8352
13	4.7421	7.5277	10.2824	11.5576	12.7599
15	4.6340	7.4270	10.1593	11.4264	12.9467
17	4.6050	7.4361	10.1237	11.3309	12.7340

**Table 7.** Convergence of the first five frequency parameters  $\Omega = \omega R_2^2 \sqrt{\rho h / D_o}$  for glass/epoxy laminated circular plate with simply supported boundary condition ( $\beta=30^\circ$ )

N	Mode number (n, s)				
	1(0,0)	2(1,0)	3(2,0)	4(0,1)	5(3,0)
(a) $h/R_2=0.1$					
7	3.5034	10.4407	18.7796	24.2754	28.9114
9	3.5393	10.1735	18.5739	24.0317	28.4791
11	3.4383	10.0711	18.3614	23.4164	27.3723
13	3.3718	9.9909	17.9813	22.9590	26.8351
15	3.4045	9.9820	17.4809	21.8198	26.5979
17	3.4005	9.8816	17.4502	21.6320	26.4817
(b) $h/R_2=0.2$					
7	3.3513	9.3009	15.6748	19.6000	22.3177
9	3.3618	9.0275	15.4348	19.4544	22.0991
11	3.2802	8.9684	15.2882	19.0893	21.5911
13	3.2426	8.9554	15.1415	18.8529	21.2247
15	3.2616	8.9813	14.7796	18.1214	21.2389
17	3.2673	8.8973	14.7225	17.9959	21.0709
(c) $h/R_2=0.3$					
7	3.1866	8.1463	12.9774	15.7974	17.5112
9	3.1831	7.8931	12.7677	15.7920	17.4032
11	3.1188	7.8659	12.6444	15.4911	17.1239
13	3.0993	7.8798	12.5900	15.3575	16.9039
15	3.1057	7.9357	12.3547	14.9203	17.0321
17	3.1145	7.8662	12.2868	14.8204	16.8499
(d) $h/R_2=0.4$					
7	3.0081	7.1210	10.8856	12.9907	14.2142
9	2.9944	6.8871	10.7105	13.0686	14.1535
11	2.9469	6.8832	10.6032	12.7802	13.9926
13	2.9399	6.9064	10.5749	12.6992	13.852
15	2.937	6.9611	10.4322	12.4442	14.0017
17	2.9456	6.9219	10.3624	12.3672	13.8266
(e) $h/R_2=0.5$					
7	2.8262	6.2571	9.2906	10.8330	11.8976
9	2.8050	6.0404	9.1440	10.9657	11.7916
11	2.7721	6.0522	9.0509	10.6362	11.7220
13	2.7741	6.0779	9.0339	10.5755	11.6313
15	2.7646	6.1150	8.9441	10.5011	11.7325
17	2.7716	6.1084	8.8769	10.4702	11.6151

**Table 8.** Convergence of the first five frequency parameter  $\Omega = \omega R_2^2 \sqrt{\rho h / D_o}$  for glass/epoxy laminated circular plate with free boundary condition ( $\beta=30^\circ$ )

N	Mode number (n, s)				
	1(2,0)	2(0,0)	3(3,0)	4(1,0)	5(4,,0)
(a) $h/R_2=0.1$					
7	3.7118	6.3054	8.3146	14.1627	15.2148
9	3.7708	6.3018	8.3498	14.1136	15.1682
11	3.6918	6.2431	8.2231	13.8570	14.6622
13	3.8405	6.4455	8.5263	14.1537	14.5310
15	3.8022	6.3160	8.5008	13.8973	14.3509
17	3.7130	6.2030	8.2279	13.7343	14.2021

**Table 8 (cont’)**. Convergence of the first five frequency parameter  $\Omega = \omega R_2^2 \sqrt{\rho h / D_o}$  for glass/epoxy laminated circular plate with free boundary condition ( $\beta=30^\circ$ )

N	Mode number (n, s)				
	1(2,0)	2(0,0)	3(3,0)	4(1,0)	5(4,,0)
(b) $h/R_2=0.2$					
7	3.5401	5.9275	7.6237	12.399	13.2206
9	3.5964	5.9130	7.6529	12.3433	13.2208
11	3.5290	5.8743	7.5478	12.1656	12.7929
13	3.6725	6.0055	7.8013	12.4383	12.7138
15	3.6219	5.8814	7.7490	12.0854	12.5366
17	3.5508	5.8334	7.5242	12.1015	12.4565
(c) $h/R_2=0.3$					
7	3.3556	5.4576	6.8876	10.7073	11.2215
9	3.4104	5.4394	6.9090	10.6440	11.2743
11	3.3337	5.3931	6.7555	10.3785	10.7682
13	3.4643	5.4529	6.956	10.6026	10.8197
15	3.4040	5.4097	6.9121	10.4271	10.7760
17	3.3517	5.3347	6.7305	10.3446	10.7459
(d) $h/R_2=0.4$					
7	3.1239	5.0220	6.0971	9.1122	9.4061
9	3.1699	5.0015	6.1170	9.0530	9.4942
11	3.1140	4.9831	6.0078	8.8975	9.1032
13	3.2316	4.9889	6.1693	9.0876	9.2664
15	3.1753	4.9471	6.1417	8.9397	9.2477
17	3.1310	4.9117	5.9955	8.897	9.1244
(e) $h/R_2=0.5$					
7	2.9136	4.6334	5.4695	7.9306	8.0256
9	2.9419	4.5941	5.4415	7.9438	7.8065
11	2.9052	4.6010	5.3842	7.8339	7.7775
13	3.0032	4.5626	5.4994	7.8039	7.8531
15	2.9521	4.5218	5.4795	7.7262	7.9618
17	2.9131	4.5104	5.3539	7.6938	7.7679

**Table 9.** Effect of varying fiber angle  $\beta$  and thickness-radius ratios  $h/R_2$ , on frequency parameter  $\Omega = \omega R_2^2 \sqrt{\rho h / D_o}$  for glass/epoxy laminated circular plate with clamped boundary condition.

$h/R_2$	$\beta$	Mode number (n, s)				
		1 (0,0)	2 (1,0)	3 (2,0)	4 (0,1)	5 (3,0)
0.1	0°	8.5546	16.6147	24.7524	29.4499	34.1353
	15°	8.5299	16.5515	24.7900	29.3319	34.1970
	30°	8.1020	15.9852	24.2492	28.3472	33.9548
	45°	7.4637	15.02533	23.4767	26.9270	33.388
	60°	6.9082	14.1306	22.7472	25.5591	32.5613
	75°	6.6518	13.5807	22.1579	24.6051	31.6929
	90°	6.6224	13.2927	21.7162	24.1544	31.1096
0.2	0°	7.5677	13.5866	19.2229	22.5626	25.3377
	15°	7.5332	13.5207	19.2428	22.4558	25.4063
	30°	7.1669	13.1066	18.9193	21.6903	25.2061
	45°	6.6354	12.4673	18.3603	20.5426	24.6637
	60°	6.1516	11.7058	17.6803	19.3599	23.9775
	75°	5.8736	11.1019	17.0165	18.4299	23.3043
	90°	5.7931	10.7894	16.5504	17.9479	22.8703

**Table 9 (cont'd).** Effect of varying fiber angle  $\beta$  and thickness-radius ratios  $h/R_2$ , on frequency parameter  $\Omega = \omega R_2^2 \sqrt{\rho h / D_o}$  for glass/epoxy laminated circular plate with clamped boundary condition.

$h/R_2$	$\beta$	Mode number (n, s)				
		1 (0,0)	2 (1,0)	3 (2,0)	4 (0,1)	5 (3,0)
0.3	0°	6.5123	10.9856	15.0768	17.5489	19.4125
	15°	6.4805	10.9345	15.1021	17.4743	19.4798
	30°	6.1890	10.6305	14.9014	16.8999	19.3194
	45°	5.7616	10.1624	14.4885	15.9917	18.8902
	60°	5.3437	9.5605	13.9163	15.0161	18.3667
	75°	5.0536	8.9877	13.3223	14.2201	17.8882
	90°	4.9334	8.6585	12.9252	13.7989	17.6097
0.4	0°	5.5909	9.0584	12.2336	14.1727	15.5552
	15°	5.5647	9.0186	12.2614	14.1189	15.6194
	30°	5.3342	8.7836	12.1203	13.6708	15.4904
	45°	4.9882	8.4219	11.7995	12.9381	15.1474
	60°	4.6260	7.9337	11.3289	12.1335	14.7456
	75°	4.3411	7.4262	10.8364	11.4702	14.4052
	90°	4.2024	7.1142	10.5202	11.1163	14.2314
0.5	0°	4.8415	7.6519	10.2403	11.8281	13.0692
	15°	4.8201	7.6184	10.2673	11.7882	12.9801
	30°	4.634	7.427	10.1513	11.4264	12.8757
	45°	4.3477	7.1339	9.8978	10.8194	12.5935
	60°	4.0316	6.7284	9.5076	10.1438	12.2749
	75°	3.7623	6.287	9.1029	9.5838	12.0243
	90°	3.6149	6.0588	8.8514	9.284	11.9136

Table 9 shows the effect of varying fiber angle  $\beta$  and thickness-radius ratios  $h/R_2$  on frequency parameters  $\Omega = \omega R_2^2 \sqrt{\rho h / D_o}$ , for glass/epoxy laminated circular plate with clamped boundary condition. It is observed that increasing the fiber orientation angle from 0° to 90° decreases the frequency parameters. This effect is larger as the thickness-radius ratios increases. The frequency parameters is observed to be maximum at fiber angle  $\beta = 0^\circ$ . The differences of fundamental frequencies between fiber angle 0° and 90° are approximately 22.58%, 23.44%, 24.24%, 24.83%, and 27.65% for  $h/R_2 = 0.1, 0.2, 0.3, 0.4$  and  $0.5$  respectively. As seen, as the thickness-radius ratios increases, the differences of fundamental frequencies increased.

**Table 10.** Effect of varying fiber angle  $\beta$  and thickness-radius ratios  $h/R_2$ , on frequency parameter  $\Omega = \omega R_2^2 \sqrt{\rho h / D_o}$  for glass/epoxy laminated circular plate with simply supported boundary condition.

$h/R_2$	$\beta$	Mode number (n, s)				
		1 (0,0)	2 (1,0)	3 (2,0)	4 (0,1)	5 (3,0)
0.1	0°	3.3775	10.0885	17.4190	22.4934	26.2291
	15°	3.3778	10.0459	17.4016	22.4156	26.2910
	30°	3.4045	9.9820	17.481	21.8198	26.5979
	45°	3.4758	9.9278	17.6586	20.9956	26.9934
	60°	3.5998	9.8639	17.7603	20.1939	27.1412
	75°	3.7438	9.705	17.5563	19.5900	26.8920
	90°	3.8368	9.4683	17.1876	19.2662	26.5024

**Table 10 (cont'd).** Effect of varying fiber angle  $\beta$  and thickness-radius ratios  $h/R_2$ , on frequency parameter  $\Omega = \omega R_2^2 \sqrt{\rho h / D_o}$  for glass/epoxy laminated circular plate with simply supported boundary condition.

$h/R_2$	$\beta$	Mode number (n, s)				
		1 (0,0)	2 (1,0)	3 (2,0)	4 (0,1)	5 (3,0)
0.2	0°	3.2695	9.0967	14.7802	18.8029	21.0527
	15°	3.2591	9.0653	14.7761	18.6957	21.1152
	30°	3.2616	8.9813	14.7796	18.1214	21.2389
	45°	3.3075	8.8860	14.8105	17.3512	21.3199
	60°	3.4045	8.7811	14.8079	16.6381	21.3604
	75°	3.5264	8.6327	14.6720	16.1170	21.3039
	90°	3.6140	8.4573	14.4608	15.8404	21.1842
0.3	0°	3.1339	8.0235	12.3738	15.4776	16.9228
	15°	3.1195	8.0141	12.3794	15.39	16.9834
	30°	3.1057	7.9357	12.3547	14.9203	17.0321
	45°	3.1253	7.8172	12.3188	14.2497	17.0024
	60°	3.1866	7.6798	12.257	13.6087	16.9916
	75°	3.2719	7.5225	12.1342	13.1368	16.9834
	90°	3.3392	7.3875	11.9952	12.8931	16.9619
0.4	0°	2.9792	7.0389	10.4565	12.8915	13.9258
	15°	2.9636	7.0355	10.4651	12.8269	14.1596
	30°	2.9370	6.9611	10.4322	12.4442	14.0017
	45°	2.9323	6.8486	10.3735	11.8704	13.9461
	60°	2.9597	6.7062	10.2885	11.3056	13.9137
	75°	3.0090	6.5418	10.1688	10.8876	13.9080
	90°	3.0536	6.4202	10.0600	10.6771	13.9157
0.5	0°	2.8171	6.1966	8.9676	10.9020	11.8000
	15°	2.8015	6.1885	8.9760	10.8693	11.8186
	30°	2.7646	6.1150	8.9441	10.5011	11.7941
	45°	2.7393	6.0132	8.8825	10.0217	11.7341
	60°	2.7382	5.8898	8.7927	9.5553	11.6953
	75°	2.7577	5.7244	8.6749	9.2076	11.6832
	90°	2.7827	5.6046	8.5798	9.0324	11.7000

Table 10 shows the effect of varying fiber angle  $\beta$  and thickness-radius ratios  $h/R_2$  on frequency parameters  $\Omega = \omega R_2^2 \sqrt{\rho h / D_o}$ , for glass/epoxy laminated circular plate with simply supported boundary condition. The fundamental frequency parameters are observed to be maximum at fiber angle  $\beta = 0^\circ$ . It is also observed that with an increase in fiber angle from  $0^\circ$  to  $90^\circ$ , it increases monotonically for thickness to radius ratio  $h/R_2=0.1$  and it decrease for the fiber angle  $0^\circ$  to  $15^\circ$ ,  $0^\circ$  to  $30^\circ$ ,  $0^\circ$  to  $45^\circ$  and  $0^\circ$  to  $60^\circ$ , for thickness-radius ratios  $h/R_2=0.2, 0.3, 0.4$  and  $0.5$  respectively and increases it afterward. The differences of fundamental frequencies between fiber angle  $0^\circ$  and  $90^\circ$  are approximately 13.59%, 10.53%, 6.55%, 2.49%, and 1.22% for  $h/R_2=0.1, 0.2, 0.3, 0.4$  and  $0.5$  respectively. As seen, as the thickness-radius ratios increases, the differences of fundamental frequencies decreases. The second (1, 0) and fourth (0, 1) frequency parameters decreases with an increase in fiber orientation angle from  $0^\circ$  to  $90^\circ$ . For thickness to radius ratios 0.1 and 0.2, third (2, 0) frequency parameters first decreases and then increases a little bit and then again decreases as the fiber angle increases. The fifth (3, 0) frequency parameters first increases and then, again decreases as the fiber angle increased.

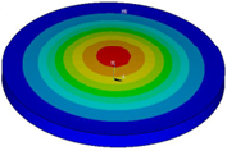
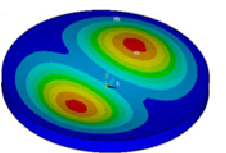
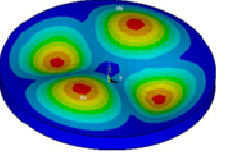
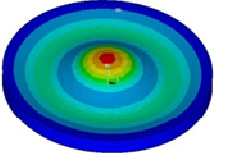
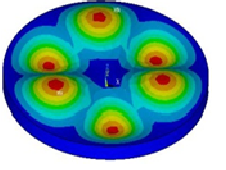
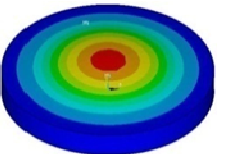
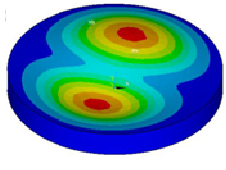
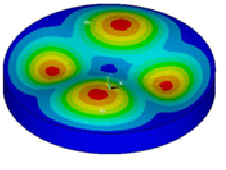
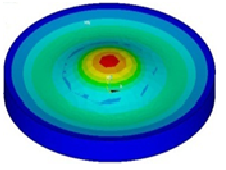
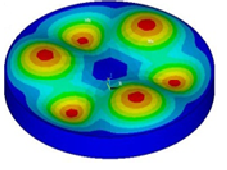
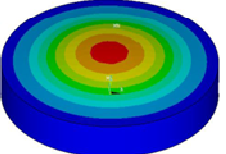
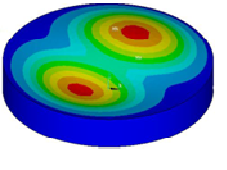
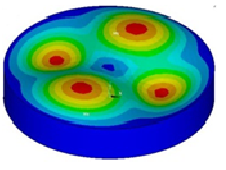
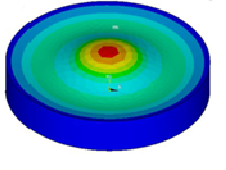
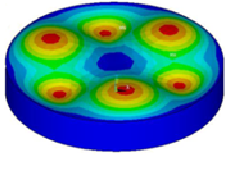
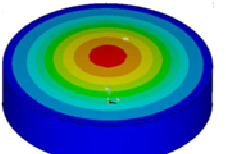
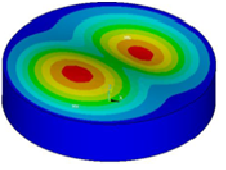
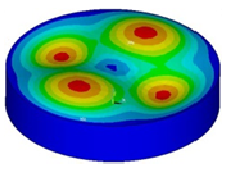
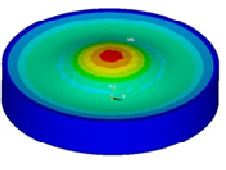
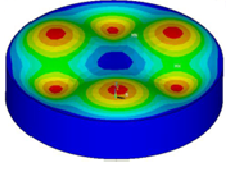
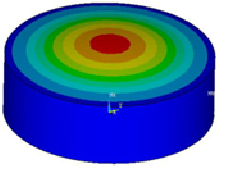
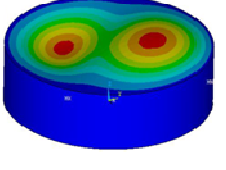
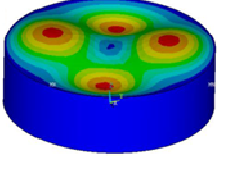
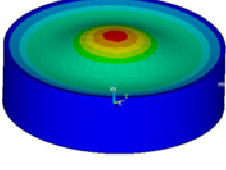
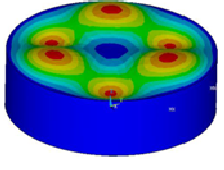
**Table 11.** Effect of varying fiber angle  $\beta$  and thickness-radius ratios  $h/R_2$ , on frequency parameter  $\Omega = \omega R_2^2 \sqrt{\rho h / D_o}$  for glass/epoxy laminated circular plate with free boundary condition.

$h/R_2$	$\beta$	Mode number (n, s)				
		1(2,0)	2(0,0)	3(3,0)	4(4,0)	5(1,0)
0.1	0°	3.7547	6.1852	8.3753	13.9372	14.6177
	15°	3.7616	6.2356	8.3823	13.8973	14.4368
	30°	3.8022	6.3160	8.5008	14.3509	13.9222
	45°	3.8834	6.4220	8.7275	14.7152	13.7542
	60°	4.0074	6.5759	9.1161	15.5451	13.7643
	75°	4.1613	6.7662	9.6596	16.7786	14.0125
	90°	4.2842	6.8771	10.1566	17.9789	14.3517
0.2	0°	3.5743	5.8201	7.6320	12.1120	12.7627
	15°	3.5816	5.8315	7.6404	12.0854	12.6293
	30°	3.6219	5.8814	7.7490	12.5366	12.1984
	45°	3.6964	5.9788	7.9504	12.7820	12.1701
	60°	3.8063	6.1079	8.2836	13.4542	12.1612
	75°	3.9501	6.2545	8.7677	14.4887	12.2446
	90°	4.0797	6.3611	9.2436	15.5233	12.4988
0.3	0°	3.3600	5.4015	6.8178	10.3369	10.8976
	15°	3.3654	5.3881	6.8191	10.3108	10.8301
	30°	3.4040	5.4097	6.9121	10.7760	10.4271
	45°	3.4734	5.4859	7.09900	10.9239	10.5106
	60°	3.5737	5.5857	7.3970	11.4726	10.5146
	75°	3.7060	5.6900	7.8155	12.3138	10.5782
	90°	3.8309	5.7859	8.2271	13.1354	10.6585
0.4	0°	3.1354	4.978	6.0656	8.8684	9.2407
	15°	3.1391	4.949	6.0603	8.8399	9.2355
	30°	3.1753	4.9471	6.1417	9.2477	8.9397
	45°	3.241	4.9992	6.3139	9.3812	9.0447
	60°	3.3348	5.0734	6.5843	9.8441	9.0638
	75°	3.4565	5.1504	6.9473	10.5376	9.0788
	90°	3.5703	5.2372	7.2928	11.1912	9.0887
0.5	0°	2.9165	4.5782	5.419	7.6801	7.963
	15°	2.9187	4.541	5.4089	7.6539	7.896
	30°	2.9521	4.5218	5.4795	7.9618	7.7262
	45°	3.0135	4.5514	5.6351	8.1441	7.8167
	60°	3.101	4.605	5.8805	8.553	7.8491
	75°	3.2129	4.6654	6.1995	9.1381	7.839
	90°	3.3153	4.7458	6.4917	9.6727	7.8082

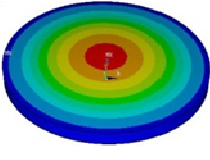
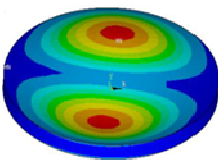
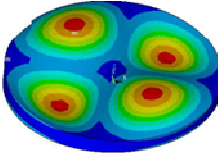
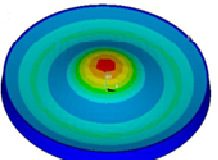
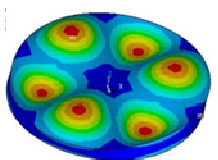
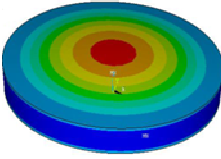
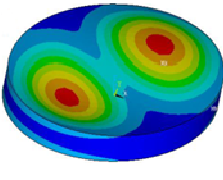
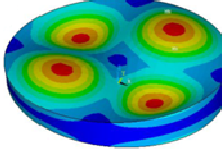
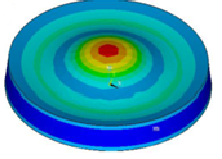
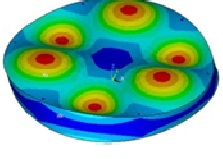
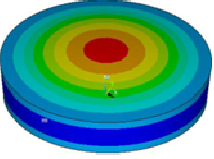
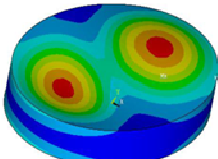
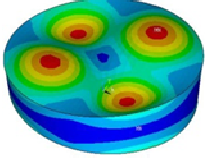
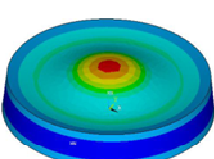
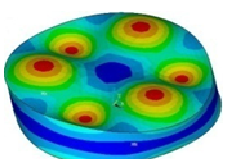
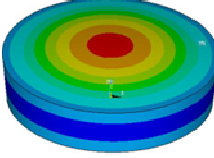
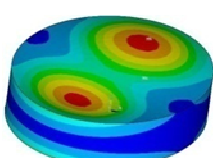
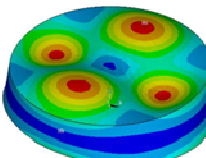
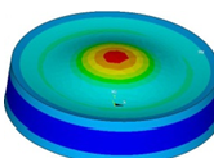
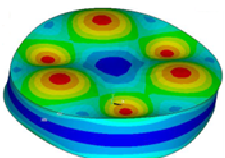
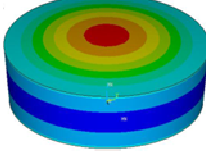
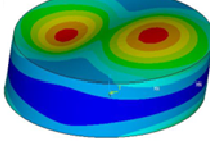
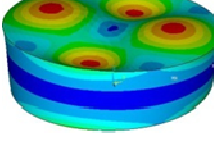
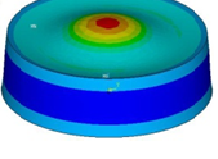
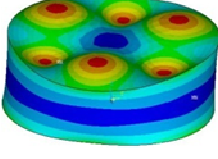
Table 11 shows the effect of varying fiber angle  $\beta$  and thickness-radius ratios  $h/R_2$  on frequency parameters  $\Omega = \omega R_2^2 \sqrt{\rho h / D_o}$ , for glass/epoxy laminated circular plate with free boundary condition. It is observed increasing the fiber orientation angle from 0° to 90° increases the frequency parameters. The fundamental frequency parameters (2, 0) are observed to be maximum at fiber angle  $\beta = 90^\circ$ . The differences of fundamental frequencies between fiber angle 0° and 90° are approximately 14.10%, 14.13%, 4.01%, 13.87%, and 13.67% for  $h/R_2 = 0.1, 0.2, 0.3, 0.4$  and  $0.5$  respectively. As seen, as the thickness-radius ratios increases, the differences of fundamental frequencies decreases. The second (0, 0) frequency parameters increase as the fiber orientation angle increases from 0° to 90°, for thickness-radius ratios  $h/R_2=0.1$  and  $0.2$  whereas, for  $h/R_2=0.3, 0.4$  and  $0.5$ , it first decreased and then increases as the fiber orientation angle increases from 0° to 90.

It is noticed that the behavior of third (3, 0) frequency parameters remains the same as that of the fundamental frequency parameters, i.e. the frequencies parameters increases as the fiber orientation angle increases from 0° to 90°. The fourth (4,0) and fifth (1,0) frequency parameters first decreased and then again, increases as the fiber orientation angle increases from 0° to 90°. Also, the first five natural modes, for the glass/epoxy laminated circular plates with clamp, simply supported and free boundary condition are shown in figure 4-6.

**Table 12.** The first five natural modes, for the glass/epoxy laminated circular plates with clamp boundary condition ( $\beta=30^\circ$ ).

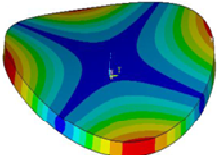
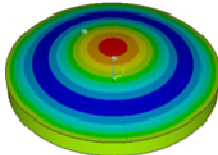
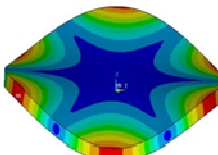
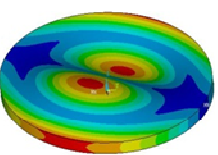
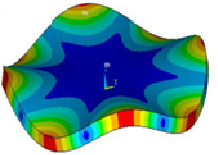
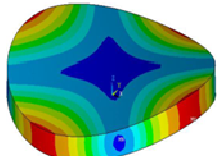
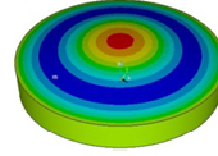
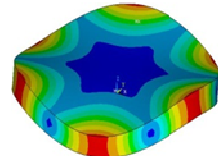
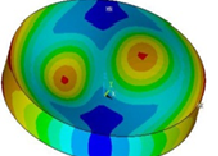
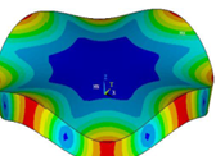
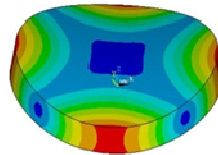
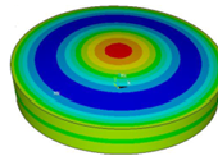
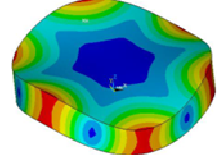
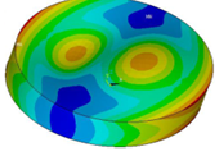
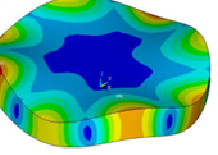
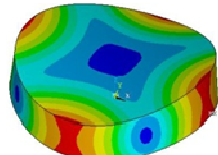
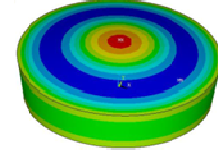
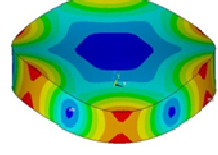
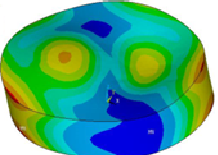
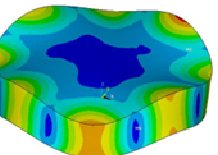
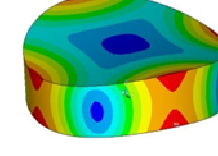
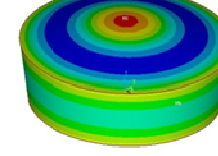
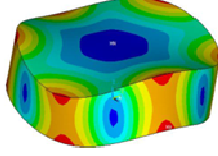
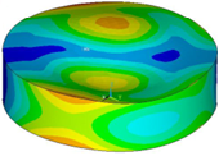
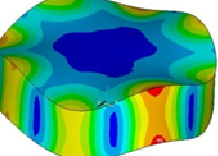
h/R <sub>2</sub>	Mode number (n, s)				
	1 (0,0)	2 (1,0)	3 (2,0)	4 (0,1)	5 (3,0)
0.1	 8.102	 8.102	 24.2492	 28.3472	 33.9548
0.2	 7.1669	 13.1066	 18.9193	 21.6903	 25.2061
0.3	 6.189	 10.6305	 14.9014	 16.8999	 19.3194
0.4	 5.3342	 8.7836	 12.1203	 13.6708	 15.4904
0.5	 4.634	 7.427	 10.1513	 11.4264	 12.8757

**Table 13.** The first five natural modes, for the glass/epoxy laminated circular plates with simply supported boundary condition ( $\beta=30^\circ$ ).

$h/R_2$	Mode number (n, s)				
	1 (0,0)	2 (1,0)	3 (2,0)	4 (0,1)	5 (3,0)
0.1	 3.4045	 9.982	 17.481	 21.8198	 26.5979
0.2	 3.2616	 8.9813	 14.7796	 18.1214	 21.2389
0.3	 3.1057	 7.9357	 12.3547	 14.9203	 17.0321
0.4	 2.937	 6.9611	 10.4322	 12.4442	 14.0017
0.5	 2.7646	 6.115	 8.9441	 10.5011	 11.7941



**Table 14.** The first five natural modes, for the glass/epoxy laminated circular plates with free boundary condition ( $\beta=30^\circ$ ).

h/R <sub>2</sub>	Mode number (n, s)				
	1 (2,0)	2 (0,0)	3 (3,0)	4 (1,1)	5 (4,0)
0.1	 3.8022	 6.316	 8.5008	 14.3509	 13.9222
0.2	 3.6219	 5.8814	 7.749	 12.5366	 12.1984
0.3	 3.404	 5.4097	 6.9121	 10.776	 10.4271
0.4	 3.1753	 4.9471	 6.1417	 9.2477	 8.9397
0.5	 2.9521	 4.5218	 5.4795	 7.9618	 7.7262

**5. Conclusions**

In this paper, a three-dimensional finite element analysis is employed for the free vibration of thick laminated composite circular plates with clamp, simply supported and free boundary condition. The effect of fiber orientation angle, thickness-radius ratios and boundary conditions on the convergence behavior was fully investigated. After comparing the present solution with the three-dimensional Ritz solution, two-dimensional Mindlin plate solution and Reddy’s third-order plate theory solution in the literature, free vibration behavior of thick laminated composite circular plates with various thickness-radius ratios was investigated. Also, first five vibration modes for different boundary conditions are shown in pictorial forms. For clamped laminated composite circular plates, fundamental frequency parameters are observed to be maximum at fiber angle  $\beta= 0^\circ$ . The fundamental frequency parameters for both simply supported and free laminated circular plate, however, is observed to be maximum at fiber angle  $\beta= 90^\circ$ . These results should be a valuable alternative for validating new computational techniques in future, due to the accuracy, simplicity and versatility of the present analysis.

## References

- Leissa A.W., 1969. *Vibration of Plates*. NASA SP-169, Office of Technology Utilization, NASA, Washington, DC.
- Rao, S. S., and Prasad, A. S., 1975. Vibrations of annular plates including the effects of rotatory inertia and transverse shear deformation. *Journal of Sound and Vibration*, Vol. 42, No 3, pp. 305-324.
- Irie, T., Yamada G., and Takagi, K., 1982. Natural frequencies of thick annular plates. *Journal of Applied Mechanics*, Vol. 49, No 3, pp.633-638.
- Han, J. B., and Liew, K. M., 1999. Axisymmetric free vibration of thick annular plates. *International Journal of Mechanical Sciences*, Vol. 41, No 9, pp. 1089-1109.
- Liew, K. M., Xiang Y. and Kitipornchai, S. 1995. Research on thick plate vibration: a literature survey. *Journal of Sound and Vibration*, Vol. 180, No 1, pp. 163-176.
- Lin, C. C., and Tseng, C. S. 1998. Free vibration of polar orthotropic laminated circular and annular plates. *Journal of Sound and Vibration*, Vol. 209, No 5, pp. 797-810.
- Kang, J. H., and Leissa, A. W., 1998. Three-dimensional vibrations of thick, linearly tapered, annular plates. *Journal of Sound and Vibration*, Vol. 217, No 5, pp. 927-944.
- So, J., and Leissa, A. W., 1998. Three-dimensional vibrations of thick circular and annular plates. *Journal of Sound and Vibration*, Vol. 209, No 1, pp. 15-41.
- Liew, K. M., and Yang, B., 1999. Three-dimensional elasticity solutions for free vibrations of circular plates: a polynomials-Ritz analysis. *Computer methods in applied mechanics and engineering*, Vol. 175, No 1, pp. 189-201.
- Liew, K. M., and Yang, B., 2000. Elasticity solutions for free vibrations of annular plates from three-dimensional analysis. *International Journal of Solids and Structures*, Vol. 37, No 52, pp. 7689-7702.
- Liew, K. M., and Liu, F. L., 2000. Differential quadrature method for vibration analysis of shear deformable annular sector plates. *Journal of Sound and vibration*, Vol. 230, No 2, pp. 335-356.
- Wu, T. Y., Wang, Y. Y., and Liu, G. R., 2002. Free vibration analysis of circular plates using generalized differential quadrature rule. *Computer Methods in Applied Mechanics and Engineering*, Vol. 191, No 46, pp. 5365-5380.
- Zhou, D., Au, F. T. K., Cheung, Y. K., and Lo, S. H., 2003. Three-dimensional vibration analysis of circular and annular plates via the Chebyshev-Ritz method. *International Journal of Solids and Structures*, Vol. 40, No 12, pp. 3089-3105.
- Wang, X., and Wang, Y., 2004. Free vibration analyses of thin sector plates by the new version of differential quadrature method. *Computer Methods in Applied Mechanics and Engineering*, Vol. 193, No 36, pp. 3957-3971.
- Hosseini-Hashemi, S., Es'Haghi, M., Taher, H. R. D., and Fadaie, M., 2010. Exact closed-form frequency equations for thick circular plates using a third-order shear deformation theory, *Journal of Sound and Vibration*, Vol. 329, pp. 3382-3396.
- Hosseini-Hashemi, S., Rezaee, V., Atashpour, S. R., and Girhammar, U. A., 2012. Accurate free vibration analysis of thick laminated circular plates with attached rigid core, *Journal of Sound and Vibration*, Vol. 331, pp. 5581-5596.
- Senjanovic, I., Hadzic, N., Vladimir, N., and Cho, D. S., 2014. Natural vibrations of thick circular plate based on the modified Mindlin theory, *Archives of Mechanics*, Vol. 66(6) , pp. 389-409.
- Sharma, A., 2014. Free vibration of moderately thick antisymmetric laminated annular sector plates with elastic edge constraints, *International Journal of Mechanical Sciences*, Vol. 83, pp.124-132.
- Powmya, A., and Narasimhan, M. C. 2015. Free vibration analysis of axisymmetric laminated composite circular and annular plates using Chebyshev collocation, *International Journal of Advanced Structural Engineering*, pp. 1-13.
- Kang, J. H., 2003. Three-dimensional vibration analysis of thick, circular and annular plates with nonlinear thickness variation. *Computers & structures*, Vol. 81, No 16, pp. 1663-1675.
- Liu, C. F., and Lee, Y. T., 2000. Finite element analysis of three-dimensional vibrations of thick circular and annular plates, *Journal of Sound and Vibration*, Vol. 233, No 1, pp. 63-80.
- Malekzadeh, P., Shahpari, S. A., and Ziaee, H. R., 2010. Three-dimensional free vibration of thick functionally graded annular plates in thermal environment. *Journal of Sound and Vibration*, Vol. 329, No 4, pp. 425-442.
- Liew, K. M., Han, J. B., Xiao, Z. M., and Du, H., 1996. Differential quadrature method for Mindlin plates on Winkler foundations. *International Journal of Mechanical Sciences*, Vol. 38, No 4, pp. 405-421.
- Zhou, D., Lo, S. H., Au, F. T. K., and Cheung, Y. K., 2006. Three-dimensional free vibration of thick circular plates on Pasternak foundation. *Journal of Sound and Vibration*, Vol. 292, No 3, pp. 726-741.
- Hashemi, S. H., Taher, H. R. D., and Omid, M., 2008. 3-D free vibration analysis of annular plates on Pasternak elastic foundation via p-Ritz method. *Journal of Sound and Vibration*, Vol. 311, No 3, pp. 1114-1140.
- Houmat, A., 2004. Three-dimensional hierarchical finite element free vibration analysis of annular sector plates. *Journal of sound and vibration*, Vol. 276, No 1, pp. 181-193.
- Komur, M. A., Sen, F., Ataş, A. , and Arslan, N. , 2010. Buckling analysis of laminated composite plates with an elliptical/circular cutout using FEM, *Advances in Engineering Software*, Vol. 41, pp. 161-164.
- Chen, D. Y., and Ren, B. S., 1998. Finite element analysis of the lateral vibration of thin annular and circular plates with variable thickness". *Journal of Vibration and Acoustics*, Vol. 120, pp. 747-752.

- Liang, B., Zhang, S. F., and Chen, D. Y., 2007 . Natural frequencies of circular annular plates with variable thickness by a new method, *International journal of pressure vessels and piping*, Vol. 84, pp. 293-297.
- Ranjan, V., and Ghosh, M.K., 2009 . Transverse vibration of spinning disk with attached distributed patch and discrete point masses using finite element analysis, *International Journal of Engineering, Science and Technology*, Vol. 1, No. 1, 2009, pp. 74-89.
- Malekzadeh, P., Afsari, A., Zahedinejad, P., and Bahadori, R., 2010. Three-dimensional layerwise-finite element free vibration analysis of thick laminated annular plates on elastic foundation, *Applied Mathematical Modelling*, Vol. 34, No 3, pp. 776-790.
- Reddy J.N., 2004. *Mechanics of Laminated Composite Plates and Shells: Theory and Analysis*. CRC Press, Boca Raton, FL, Second Edition.
- ANSYS Inc., 2009. *ANSYS 12.0 reference manual*.

#### **Biographical notes**

**Dr N. D. Mittal** is a faculty member in the department of Mechanical Engineering, Maulana Azad National Institute of Technology, Bhopal

**Sumit Khare** is research student in the department of Mechanical Engineering, Maulana Azad National Institute of Technology, Bhopal.

Received November 2015

Accepted March 2016

Final acceptance in revised form June 2016